X-ray Diffraction Study of Lithium Hydrazinium Sulfate and Lithium Ammonium Sulfate Crystals Under a Static Electric Field

By M. T. Sebastian, R. A. Becker & H. Klapper*

Institut für Kristallographie, RWTH, 5100 Aachen, Germany

Abstract

X-ray diffraction studies are made on proton-conducting polar lithium hydrazinium sulfate and ferroelectric lithium ammonium sulfate. The X-ray rocking curves recorded with *in situ* electric field along the polar *b* axis of lithium hydrazinium sulfate (direction of proton conductivity) show a strong enhancement of the $0k0$ diffraction intensity. The corresponding $0k0$ X-ray topographs reveal extinction contrast consisting of striations parallel to the polar axis. They disappear when the electric field is switched off. The effect is very strong in $0k0$ but invisible in $h0l$ reflections. It is present only if the electric field is parallel to the polar axis *b*. This unusual X-ray topographic contrast is correlated with the proton conduction. It is supposed that, under electric field, an inhomogeneous charge distribution develops, distorting the crystal lattice. Similar experiments on lithium ammonium sulfate also show contrast variations, but of quite different behaviour than before. In this case they result from changes of the ferroelectric domain configuration under electric field.

1. Introduction

Lithium hydrazinium sulfate ($LiN_2H_5SO_4$, LHzS) and lithium ammonium sulfate ($LiNH_4SO_4$, LAS) crystallize under ambient conditions in the polar space group $Pc2_1n$. Their structures have been studied by X-ray and neutron diffraction (Brown, 1964; Van den Hende & Boutin, 1964; Padmanabhan & Balasubramanian, 1967; Dollase, 1969). Both structures consist of a framework of alternately linked LiO_4 and SO_4 tetrahedra of the *Icmm* type (Chung, 1972; Hildman, 1980). The $N_2H_5^+$ and NH_4^+ ions are located in the framework channels which define the polar axis.

In LHzS the N—N bond axis of the $N_2H_5^+$ ions is normal to the channel direction **b** (Fig. 1). The two protons of the NH_2^+ group form hydrogen bonds,

one to an oxygen, the other to the next nitrogen in the channel, whereas the NH_3^+ groups nestle in the cavities in the negatively charged $LiSO_4$ framework (Fig. 1). Thus hydrogen-bonded ···N—H···N—H··· N—H··· chains are formed in the channels. They allow the transfer of protons from one nitrogen to another. This explains the high electrical (proton) conductivity along the polar *b* axis (Vanderkooy, Cuthbert & Petch, 1964; Brown, 1964; Lundgren, Liminga & Olovsson, 1968). More recently the dynamics of the proton transfer has been explained by a vehicular mechanism where $N_2H_5^+$ is responsible for carrying the protons (Kreuer, Weppner & Rabenau, 1981; Kreuer, Rabenau & Weppner, 1982). LHzS was suspected to be ferroelectric at room temperature (Pepinsky, Vedam, Okaya & Hoshino, 1958). This, however, could not be confirmed by X-ray topography, etching and piezoelectric studies which proved the absence of ferroelectric 180° domains (inversion twins) in all crystals (Wardani, 1978; Klapper & Wardani, 1978). The untypical hysteresis loop (erroneously interpreted as ferroelectricity) arises from a saturation of the AC conductivity (Schmidt & Drumheller, 1971).
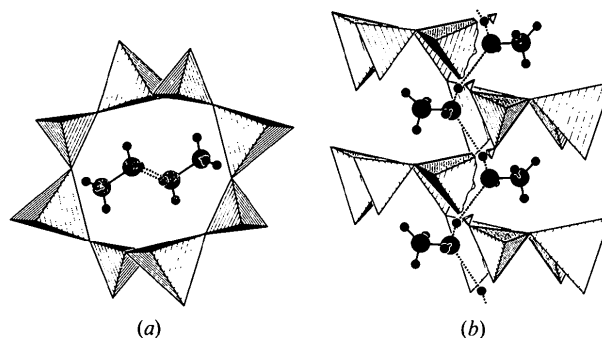

Fig. 1. Fragment of the $LiSO_4$ tetrahedral framework showing one channel containing the hydrogen-bonded N_2H_5 chain. Small tetrahedra: SO_4, large tetrahedra: LiO_4. (*a*) View along the polar axis. The N_2H_5 chain is projected 'end-on'. (*b*) View normal to the polar axis, showing the zig-zag arrangement of the N_2H_5 chains. The hydrogen bonds along the chain are indicated by dotted lines. The drawings were performed using the program *STRUPLO* (Fischer, 1985).

---

* Present address: Mineralogisches Institut, Universität Bonn, 5300 Bonn, Germany.

No proton conductivity occurs in LAS which, however, is ferroelectric in the temperature range between 283 and 459 K (Mitsui, Oka, Shiroshi, Takashigi, Ito & Sawada, 1975; Aleksandrov, Aleksandrov, Zherebsova, Kruglik, Krupnyj, Melnikova, Schneider & Shuvalow, 1975). The as-grown crystals contain 180° domains (inversion twins) in the shape of thin (001) lamellae (Klapper, 1987; Hildmann, Klapper & Hahn, 1978). The ferroelectric domain configuration in LAS has been observed at room temperature by pyroelectric probe (Gerbaux, Mangin, Hadni, Perrin & Tran, 1982), scanning and transmission electron microscopy (Hilczer, Meyer & Szczesniak, 1984; Mausson, Polomska & Le Bihan, 1986) and by etching and X-ray topography (Hildmann et al., 1978; Klapper, 1987; Jennissen, 1990). Recently Polomska & Tikhomirova (1982) observed the domain patterns in liquid-crystal-decorated LAS under a DC electric field. The as-grown domain structure is reported to change during mild heating (Mitsui, Oka, Shiroshi, Takashigi, Ito & Sawada, 1975; Jennissen, 1990).

The inversion twin domains have exactly parallel lattices reflecting X-rays with the same structure-factor modulus. Hence no domain contrast will be observed on the topographs. However, the domain boundaries become visible on X-ray topographs by a fringe pattern which corresponds to that commonly observed for stacking faults (Klapper, 1987). The dislocation arrangements and microhardness properties of both crystals, LHzS and LAS, were studied by Wardani (1978) and Klapper & Wardani (1978).

In the present paper we report an increase of diffracted X-ray intensity by reduced extinction and the generation of new topographic contrast in LHzS and LAS under the influence of an electric field along the polar axis. A similar investigation has been performed by the authors on α-lithium iodate (Sebastian, Klapper & Haussühl, 1989). An earlier X-ray topographic study of defects in ionic conducting crystals under the action of an electric DC field is reported by Gu, Ge, Zhao, Hu, Wu & Fu (1980).

2. Experimental

Large single crystals (up to 5 cm diameter) of LHzS and LAS were grown on seed crystals from aqueous solution by evaporation at 313 K. The solutions were prepared by dissolving equimolar fractions of Li_2SO_4, $(N_2H_5)_2SO_4$ and $(NH_4)_2SO_4$.

Thin plates of orientations (100), (001) and (101), approximately 1 mm thick, were cut with a string saw and polished on soft wet tissue. A static electric field of 1–8 kV cm^{-1} was applied in various crystallographic directions parallel to the specimen plates using soft graphite electrodes. The soft graphite electrodes (cut from a graphite felt obtained from Sigri

GmbH, Meitingen, Germany) make very good electrical contact also with curved crystal edges. We have avoided using silver paste electrodes since it is known (Keerti & Lang, 1972) that silver ions migrate into the crystal lattice during solid-state electrolysis. X-ray rocking curves and X-ray topographs were recorded in situ using Mo $K\alpha$ radiation (linear absorption coefficient $\mu = 0.60$ mm^{-1} for LHzS and $\mu = 0.64$ mm^{-1} for LAS). The experimental set-up, which was mounted on a commercial Lang camera, is outlined in Fig. 2. For section topographs a collimating slit of 10 μm width was used.

3. Results

Lithium hydrazinium sulfate

Fig. 3 represents a typical sequence of 020 reflection rocking curves recorded with increasing electric field along the polar axis. For zero field, the reflected intensity is, due to high extinction, low. The $K\alpha_{1,2}$ splitting is clearly visible. With increasing field the diffracted intensity increases strongly, reaching a value about ten times higher for 8 kV cm^{-1} than for the field-free case. Simultaneously, the $K\alpha_{1,2}$ splitting is blurred due to a broadening of the reflection range. There is no significant shift of the peak centre due to the field.

The intensity increase does not appear instantaneously on applying the field. It reaches its maximum (saturation) after a few seconds. The intensity relaxation after switching off the field is much slower; it takes about one minute to come back to the original zero-field value. It is noted that the sample was not short-circuited in these studies. For short-circuiting a shorter relaxation time is expected. If, however, a high electric field (> 1 kV cm^{-1}) is applied for a long time (> 1 h), the intensity returns to a value higher than the original. The 'new' intensity is stable and does not relax with
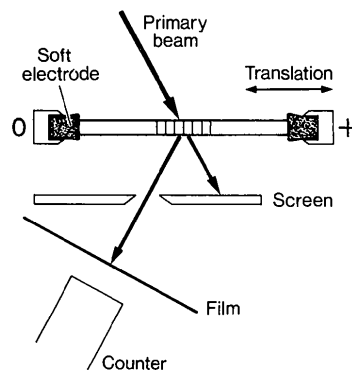

Fig. 2. Schematic sketch of the experimental set-up to record the X-ray rocking curves and topographs with in situ electric field.

time. This indicates that an irreversible change of crystal perfection, proven by reduced extinction, has occurred. If the rocking curves are recorded in reflections $h0l$ (*i.e.* reflecting planes parallel to the polar axis and the electric field), no intensity change is observed. If the field is applied normal to the polar axis, no effect occurs, either in $0k0$ or $h0l$ reflections.

More detailed information on the intensity increase is given by X-ray transmission topography. Fig. 4 presents a typical sequence of 020 topographs with various *in situ* electric fields. It is noted that the soft electrodes were attached under slight pressure to the irregularly formed right and left edges of the plate, which provide sufficient electrical contact to all segments of the side edges. Due to low absorption of the soft graphite wool, the X-ray intensity reflected from the edge regions is not modified.

Fig. 4(*a*) shows a (101) plate before applying the electric field. Grown-in and mechanical defects as well as *Pendellösung* fringes are visible. After applying a field of 1 kV cm^{-1} along the polar axis, inhomogeneous striation contrasts appear along this direction (Fig. 4*b*). On further increase of the field to 2 kV cm^{-1}, the striations become denser, more homogeneous and more intense (Fig. 4*c*). It is noted that the overall reflected intensity is increased by a factor of about 4, *i.e.* the exposure time of Fig. 4(*c*) is
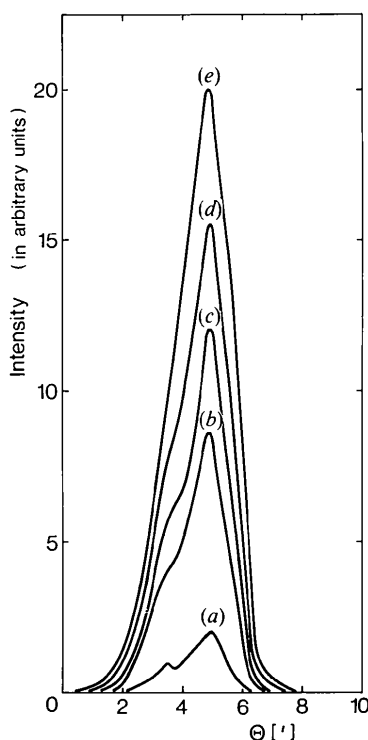
only about one quarter of that of topograph Fig. 4(*a*). After switching off the field, the original topograph appears again, however with irreversible additional defects of dotty appearance arranged in rows along the polar axis. These 'new' defects are obviously precipitates arising from local decomposition of LHzS under an electric field (see *Discussion*). The reversal of the electric field to -2 kV cm^{-1} (Fig. 4*e*) generates essentially the same striation contrast [compare with Fig. 4(*c*): $+2$ kV cm^{-2}], though the two directional senses of the polar axis are physically different and differences between topographs in Figs. 4(*c*) and (*e*) could be expected.

After several hours under high electric field (> 1 kV cm^{-1}), the decomposition of LHzS has further proceeded as is demonstrated in the topograph in Fig. 4(*f*) taken without electric field after several high-voltage experiments. Now many precipitates lined up in rows parallel to the polar axis have formed.

The striation contrast observed in Figs. 4(*b*), (*c*), (*e*) exhibits a characteristic 'extinction behaviour'. It is strong in reflection 020 (reflecting planes normal to the polar axis) and invisible (extinct) in reflections $h0l$ (reflecting planes parallel to the polar axis), provided that decomposition has not yet started (see *Discussion*). For electric fields normal to the polar axis, no striations or intensity variations are found, whichever reflection was used for imaging.

Fig. 5 shows a sequence of 020 section topographs recorded from the same part of a (101) LHzS plate without and with electric field along the (horizontal) polar axis. The crystal was subjected to an electric field for a short interval before recording Fig. 5(*a*). Despite some previously generated defects, *Pendellösung* fringes are visible in Fig. 5(*a*), indicating good crystalline quality. The electric field (Figs. 5*b*, *c*) induces many contrast spots arising from the interior of the crystal, and a strong intensity enhancement from regions close to one of the plate surfaces (left side of section topographs) appears. Most of these contrasts vanish after switching off the electric field (Fig. 5*d*). Some, however, are due to decomposition and remain.

LHzS suffers X-radiation damage. This is demonstrated in Fig. 6 which shows increased diffracted intensity arising from the region previously irradiated for 30 min in order to record a section topograph.

Fig. 3. 020 rocking curves recorded with and without *in situ* electric field along the polar axis. (*a*) $E = 0$, (*b*) $E = 2$ kV cm^{-1}, (*c*) $E = 4$ kV cm^{-1}, (*d*) $E = 6$ kV cm^{-1}, (*e*) $E = 8$ kV cm^{-1}.

Lithium ammonium sulfate

The intensity changes of the 020 reflection of LAS due to electric field along the polar axis are quite different from those observed for LHzS. They appear instantaneously with application of the electric field and may be an increase or a decrease. Even if the

field is kept constant for some minutes, sudden intensity variations appear during this period. A plot of the 020 intensity *versus* time with electric field variations is shown in Fig. 7.

It is obvious that these intensity changes result from changes of ferroelectric domains, which can be considered as 'inversion twins'. Owing to Friedel's law, however, the intensity variations cannot arise from the polarity change in the volume, but from the alteration of twin (domain) boundaries which generate strong contrast on X-ray topographs. This is

demonstrated in the series of topographs in Fig. 8. Fig. 8(*a*) shows the plate in virginal state exhibiting the known grown-in defects of LAS including the (001) twin lamellae. In the later zero-field topographs in Figs. 8(*c*) and (*e*), the domains are significantly changed. The *in situ* field topographs, Figs. 8(*b*), (*d*), (*f*), show many diffuse and strong contrasts. They may also result from inhomogeneous electrostrictive strain. Dislocations are not changed by the electric field. Additional information on the changes of domain is gained from section topographs. Fig. 9
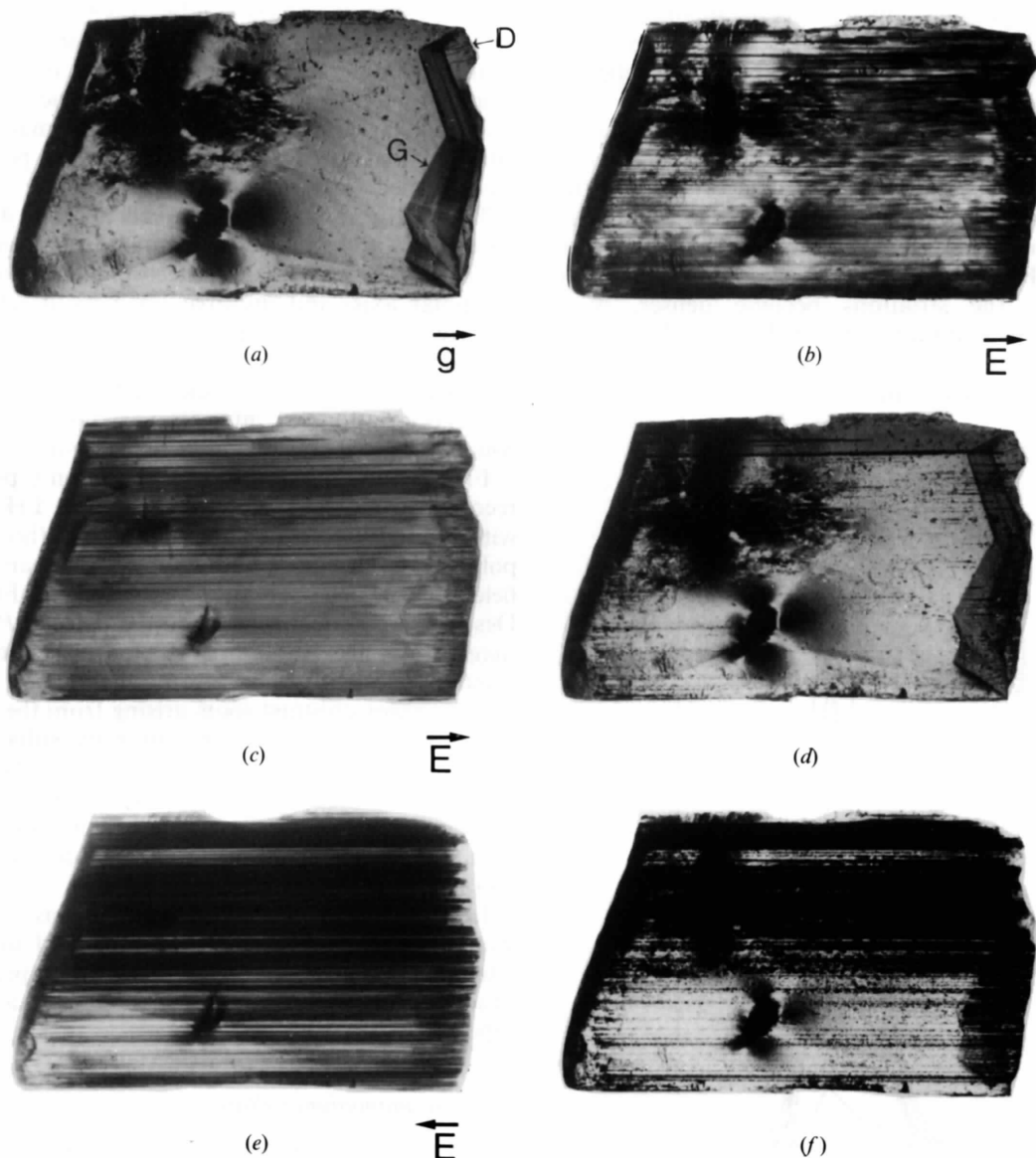

Fig. 4. Sequence of 020 X-ray topographs of a (101) LHzS plate, horizontal dimension 25 mm and thickness 1 mm, recorded with *in situ* electric fields of various strengths along the polar axis, *b*. (*a*) No field. The topograph shows grown-in defects (growth-sector boundary *G*, dislocation bundles *D* penetrating the plate). *Pendellösung* fringes prove high local perfection. (*b*) $E = 1$ kV cm^{-1}, (*c*) $E = 2$ kV cm^{-1}, (*d*) no field, (*e*) $E = -2$ kV cm^{-1}, (*f*) no field, after several hours of applying various electric fields.

presents 020 section topographs recorded from the same part of a (101) plate. In Fig. 9(a) (no electric field) laterally restricted grown-in domain lamellae (intersecting the plate under 40°) are recognized. Under the electric field of -2 kv cm^{-1} (Fig. 9b) these domains have nearly completely vanished, but other diffuse contrasts partially extending from the surface into the bulk appear. Fig. 9(c) was recorded without electric field. The drastic change of domain configuration to a higher density of lamellae as compared with Fig. 9(a) is apparent.

4. Discussion

Lithium hydrazinium sulfate

There is no doubt that the intensity increase of the 020 reflections and the striation contrasts of 020 topographs have their origin in the (proton) conductivity of LHzS. Exactly the same intensity changes and the same contrast features including the extinction behaviour of field-induced striations are observed in Li-conducting lithium iodate (Bouillot,

Baruchel, Remoissenet, Joffrin & Lajzerowicz, 1982; Sebastian, Klapper & Haussühl, 1989; Li, 1985; Liang & Li, 1978) and K-conducting KTiOPO$_4$ (KTP) (Sebastian, Klapper & Bolt, 1992), but not in non-conducting and non-ferroelectric potassium lithium sulfate KLiSO$_4$. Neutron diffraction intensities are affected too: Yang, Niu & Cheng (1979) report that the intensities of neutrons diffracted from lithium iodate (reflection 002) are enhanced by more than one order of magnitude under the action of even a moderate electric field. The enhancement may vary from one sample to another.

The drastic increase of diffraction intensities and the appearance of striation contrast is a phenomenon which seems to be characteristic of ionically conducting polar crystals. It is assumed that the motion of ions (protons in the case of LHzS) leads to an inhomogeneous charge distribution which generates, for example by electrostrictive forces, distortions of the crystal lattice and, as a consequence, an increase of diffracted intensity. These distortions are such that the lattice displacements are parallel to the polar axis which is the direction of the electric field. Under this aspect striations show the same contrast behaviour as pure screw dislocations. Of course, they are not dislocations (which cannot appear and vanish reversibly with the electric field). On the other
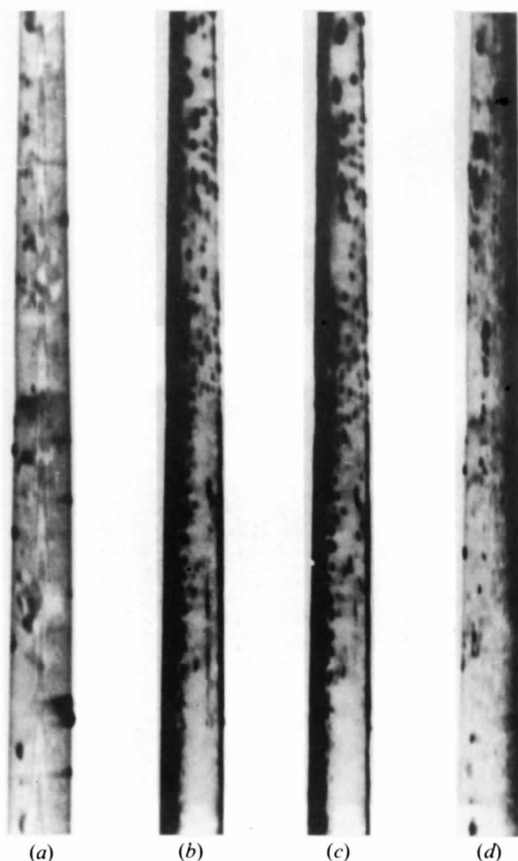

Fig. 5. 020 section topographs of a (101) plate recorded with in situ electric fields of various strengths along the polar axis. (a) $E = 0$, (b) $E = 1$ kV cm^{-1}, (c) $E = 2$ kV cm^{-1}, (d) $E = 0$.
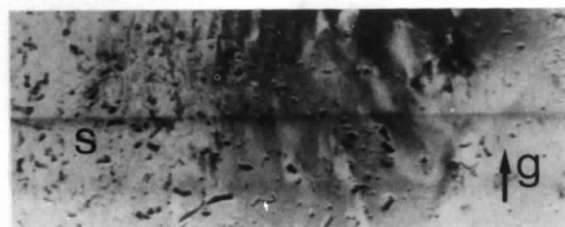

Fig. 6. 020 transmission topograph of a (101) plate. The line with enhanced intensity (radiation damage) shows the region where a section topograph was recorded previously.
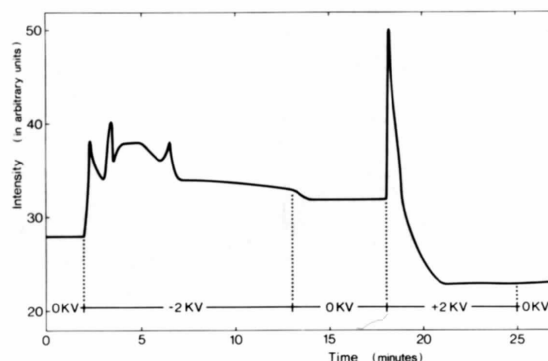

Fig. 7. Plot of the diffracted X-ray intensity versus time for the 020 reflection from a LAS crystal with in situ electric fields along the b axis.

hand, single striations cannot be identified with single framework channels (or H-bonded N_2H_5 chains) though strong correlation between the two apparently exists. Thus, the mechanism leading to the striation contrast on 020 topographs is not yet fully understood.
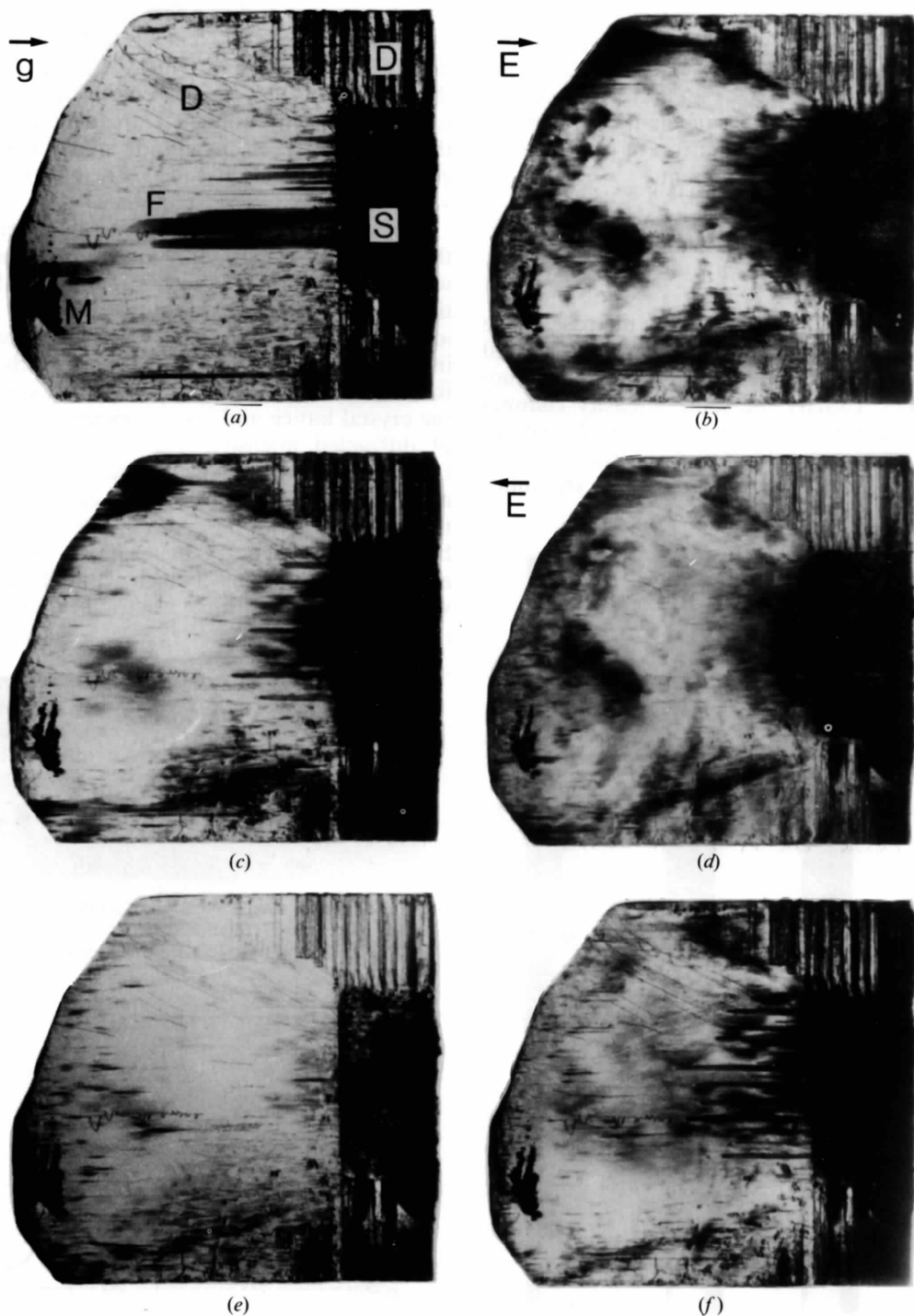

Fig. 8. Sequence of 020 transmission topographs of a (101) LAS plate (14 × 12 mm, about 1 mm thick) recorded with *in situ* electric field of various strengths along the polar (ferroelectric) axis. (*a*) $E = 0$. *S*: seed crystal; *D*: dislocations; *F*: inversion twin lamellae (ferroelectric domains), intersecting the plate under about 40°; *M*: mechanical surface defect. (*b*) $E = -1.5$ kV cm^{-1}, (*c*) $E = 0$, (*d*) $E = 1.5$ kV cm^{-1}, (*e*) $E = 0$, (*f*) $E = 0$ (recorded after applying -1.5 kV cm^{-1} for 2 h).

On section topographs the striations appear as spots (Figs. 5b, c). The intensity increase from regions close to one of the plate surfaces (Figs. 5b, c) is not understood. A similar result has been reported by Baruchel, Bouillot & Coquet, 1991), who observed on section topographs of α-LiIO$_3$ under *in situ* electric field an intensity enhancement, which is associated with fine line contrast originating from crystal regions close to both plate surfaces. It is possible that this effect is due to a higher surface electrical conduction.

LHzS is thermally unstable. It can decompose into neutral hydrazine N$_2$H$_4$ and LiHSO$_4$. Indeed, a loss of hydrazine from LHzS at temperatures above 353 K was found by Kreuer *et al.* (1981). The same authors mention that an electrolytical decomposition starts a low DC voltage of 35 mV at 353 K. It is assumed that the decomposition and precipitation appearing on the topographs of LHzS crystals exposed to high electric fields are of the same kind as described by Kreuer, Weppner & Rabenau (1981) and Kreuer, Rabenau & Weppner (1982). It is an interesting feature that these precipitates line up in rows parallel to the conduction axis. These rows are correlated with those striations of particularly high intensity, which obviously act as sources of preferred precipitation.

Similar effects of X-ray intensity enhancement and striation contrast under the action of an electric field occur in α-quartz (Calamiotou, Psicharis, Filippakis & Anastassakis, 1987; Gouhara, Bessho, Yasuda & Kato, 1982; Sebastian, Zarka & Capelle, 1988). Here the effect is present in all *hkl* topographs and is reported (Sebastian *et al.*, 1988; Sebastian & Klapper, 1990) to be due to negative space charges which develop at the anode side of the specimen and deform the crystal lattice. The negative space charges result from the detraction of those alkali ions (mostly Na$^+$ and Li$^+$) which compensate for the lower valency of Al^{3+} substituting for Si^{4+}.

Lithium ammonium sulfate

It is the essential and defining feature of ferroelectricity that ferroelectric domains are changed under electric field. Thus, the change of domains toward the single-domain state of LAS under an electric field is quite normal. The reappearance of domains after removing the field is also quite normal, since the single-domain state is not stable without field. What, however, is surprising is the drastic increase of domain density after switching off the *E* field at room temperature within a short time (Fig. 9c). This is in contradiction to the observed stability of the grown-in domain configurations with much less density of lamellae. Another point of interest is that LAS is a 'hard' ferroelectric at room temperature with a coercive field of 51 kV cm^{-1} at 303 K (Mitsui *et al.*, 1975). Under this aspect a switching of domains in LAS should be impossible under those comparatively moderate fields of our experiments. It should, however, be noted that in usual experiments the polar axis and the electric field are oriented normal to the specimen plate, whereas in our present study they are parallel to the plate. In our case the depolarizing field is lower than in the former case. This may explain that the single-domain state is reached for relatively low electric fields. Moreover, the effect of the surfaces (which are, due to etch patterns, not planar) is strong, leading to high field inhomogeneities which may influence the domain switching and configurations. The diffuse contrasts arising under electric field and originating mostly from the surface (see section topograph Fig. 9b) may also result from such field inhomogeneities, due to electrostrictive effects. Thus the switching behaviour of ferroelectric domains in LAS is not yet fully
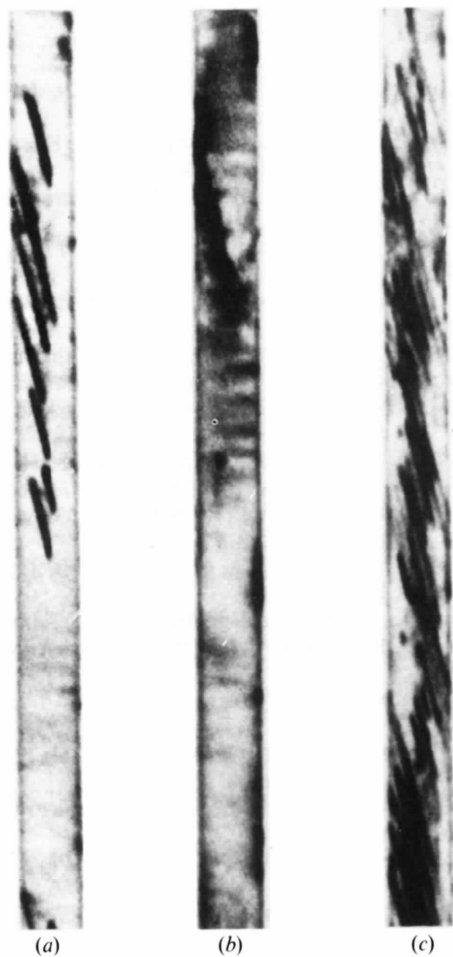

(a)   (b)   (c)

Fig. 9. 020 section topographs of a (101) LAS plate. (a) $E = 0$, (b) $E = -2$ kV cm^{-1} along the polar axis, (c) $E = 0$.

understood and requires a more detailed investigation, which will be performed in the near future.

In conclusion, it is mentioned that an enhancement of the diffracted X-ray intensity under high AC and DC electric fields has been observed in the following crystals which are not ion conducting: silicon (Lal & Thoma, 1983; Lal, 1988), KDP [neutron diffraction (Sedlakova, Petrzilka, Mikula, Chalupa, Michhalic & Cech, 1975) and TGS [neutron diffraction (Yang, Cheng & Niu, 1978)]. For KDP and TGS the effect is attributed to piezoelectric (electrostrictive) interactions, in silicon it is assumed to be associated with structural and compositional inhomogeneities which are present as unavoidable point defects and their clusters. Recently, Bhasin, Kothari, Lal & Srivastava (1988) and Pietsch & Unger (1978) attributed the effect to variations in the electron density distribution and the bond charge. Other crystals tested by Yang *et al.* (1979), KLiSO₄, TiO₂, LiNbO₃ and NaCl, did not show significant intensity changes under the action of an electric field.

References

ALEKSANDROV, K. S., ALEKSANDROV, I. P., ZHEREBSOVA, L. I., KRUGLIK, A. I., KRUPNYJ, A. I., MELNIKOVA, S. V., SCHNEIDER, V. P. & SHUVALOW, L. A. (1975). *Izv. Akad. Nauk SSSR Ser. Fiz.* **39**, 943.

BARUCHEL, J., BOUILLOT, J. & COQUET, E. (1991). *Philos. Mag.* **B63**, 1051–1062.

BHASIN, V. S., KOTHARI, L. S., LAL, K. & SRIVASTAVA, M. P. (1988). *Phys. Lett. A*, **133**, 438–439.

BOUILLOT, J., BARUCHEL, J., REMOISSENET, M., JOFFRIN, J. & LAJZEROWICZ, J. (1982). *J. Phys. (Paris)*, **43**, 1259–1266.

BROWN, B. D. (1964). *Acta Cryst.* **17**, 654–660.

CALAMIOTOU, M., PSICHARIS, V., FILIPPAKIS, S. E. & ANASTASSAKIS, E. (1987). *J. Phys. C*, **20**, 5641–5653.

CHUNG, S. J. (1972). Thesis, Technical Univ. of Aachen, Germany.

DOLLASE, W. A. (1969). *Acta Cryst.* **B25**, 2298–2302.

FISCHER, R. X. (1985). *J. Appl. Cryst.* **18**, 258–262.

GERBAUX, X., MANGIN, J., HADNI, A., PERRIN, D. & TRAN, C. T. (1982). *Ferroelectrics*, **40**, 53–59.

GOUHARA, K., BESSHO, Y., YASUDA, K. & KATO, N. (1982). *Jpn. J. Appl. Phys.* **21**, L503–504.

GU, Y., GE, P., ZHAO, Y., HU, B., WU, L. & FU, Q. (1980). *Acta Phys. Sin.* **29**, 711–715.

HILCZER, B., MEYER, K.-P. & SZCZESNIAK, L. (1984). *Ferroelectrics*, **55**, 201–204.

HILDMANN, B. O. (1980). Thesis, Technical Univ. of Aachen, Germany.

HILDMANN, B. O., KLAPPER, H. & HAHN, TH. (1978). *Z. Kristallogr.* **146**, 153–154.

JENNISSEN, H.-D. (1990). Thesis, Technical Univ. of Aachen, Germany.

KEERTI, S. & LANG, A. R. (1972). *J. Appl. Cryst.* **5**, 72–78.

KLAPPER, H. (1987). In *Progress in Crystal Growth and Characterization*, Vol. 14, edited by P. KRISHNA & B. PAMPLIN. Oxford: Pergamon.

KLAPPER, H. & WARDANI, A. M. (1978). *Acta Cryst.* **A34**, S243.

KREUER, K. D., RABENAU, A. & WEPPNER, W. (1982). *Angew. Chem. Int. Ed. Engl.* **21**, 208.

KREUER, K. D., WEPPNER, W. & RABENAU, A. (1981). *Solid State Ion.* **3/4**, 353–358.

LAL, K. (1988). *Rigaku J.* **5**, 11–24.

LAL, K. & THOMA, P. (1983). *Phys. Status Solidi A*, **80**, 491.

LI, Y. (1985). In *Advances in Sciences of Chinese Physics*, Vol. 1, pp. 45–78. Beijing: Science Press.

LIANG, J. & LI, S. (1978). *Acta Phys. Sin.* **27**, 126–136.

LUNDGREN, J., LIMINGA, R. T. & OLOVSSON, I. (1968). *Ark. Kemi*, **30**, 81.

MAUSSON, M., POLOMSKA, M. & LE BIHAN, R. (1986). *Ferroelectrics Lett.* **6**, 41–46.

MITSUI, T., OKA, T., SHIROSHI, Y., TAKASHIGI, M., ITO, K. & SAWADA, S. (1975). *J. Phys. Soc. Jpn*, **39**, 845–846.

PADMANABHAN, V. M. & BALASUBRAMANIAN, R. (1967). *Acta Cryst.* **22**, 532–537.

PEPINSKY, R., VEDAM, K., OKAYA, Y. & HOSHINO, S. (1958). *Phys. Rev.* **111**, 1467–1468.

PIETSCH, U. & UNGER, K. (1978). *Phys. Status Solidi B*, **143**, K95–K96.

POLOMSKA, M. & TIKHOMIROVA, A. (1982). *Ferroelectrics Lett.* **44**, 205–211.

SCHMIDT, V. H. & DRUMHELLER, J. E. (1971). *Phys. Rev. B*, **4**, 4582.

SEBASTIAN, M. T. & KLAPPER, H. (1990). 4th Eur. Time and Frequency Forum, Neuchatel, Switzerland.

SEBASTIAN, M. T., KLAPPER, H. & BOLT, R. J. (1992). *J. Appl. Cryst.* Submitted.

SEBASTIAN, M. T., KLAPPER, H. & HAUSSÜHL, H. (1989). In *Materials for Non-linear and Electro-optics*, edited by M. H. LYONS. *Inst. Phys. Conf. Ser.* No. 103, pp. 53–58. Bristol: Institute of Physics.

SEBASTIAN, M. T., ZARKA, A. & CAPELLE, B. (1988). *J. Appl. Cryst.* **21**, 326–329.

SEDLAKOVA, L., PETRZILKA, V., MIKULA, P., CHALUPA, B., MICHHALIC, R. & CECH, J. (1975). *Phys. Status Solidi A*, **27**, 309.

VAN DEN HENDE, J. H. & BOUTIN, H. (1964). *Acta Cryst.* **17**, 660–663.

VANDERKOOY, J., CUTHBERT, J. D. & PETCH, H. E. (1964). *Can. J. Phys.* **42**, 1871–1878.

WARDANI, A. M. (1978). Diplomarbeit, Technical Univ. of Aachen, Germany.

YANG, Z., CHENG, Y. & NIU, S. (1978). *Acta Phys. Sin.* **27**, 226–228.

YANG, Z., NIU, S. & CHENG, Y. (1979). *Sci. Sin.* **22**, 1000–1009.